gAAA-3′) or an ISRE radiolabeled probe (5′-gATCgggAAAgggAAACCgAAACTgAA-3′). The signal was quantified with a phosphorimager (Amersham).
15. SV40 fibroblasts, unstimulated or stimulated with IFN-γ or IFN-α for 30 min, were fixed with 3% paraformaldehyde or 100% methanol at −20°C and permeabilized with 0.1% Triton X-100 (Sigma). The fibroblasts were incubated with mouse monoclonal antibody to STAT-1 (N-Terminus; Transduction Laboratories) or rabbit antibody to STAT-2 (sc476; Santa Cruz) for 30 min, followed by fluorescein isothiocyanate (FITC)–conjugated antibody to mouse or antibody to rabbit for 30 min (Jackson).
16. C. V. Ramana, M. Chatterjee-Kishore, H. Nguyen, G. R. Stark, *Oncogene* **19**, 2619 (2000).
17. Lysates from EBV-B cells, either not stimulated or stimulated with IFN-α or IFN-γ for 30 min, were immunoprecipitated with a monoclonal antibody to STAT-1 IgG1 (Sc417; Santa Cruz). Immune complexes were analyzed by 8% SDS–polyacrylamide gel electrophoresis (SDS-PAGE) and Western blotting. The polyvinylidene fluoride membrane was probed with a rabbit antibody to phosphotyrosine 701–STAT-1 (9171L; New England Biolabs) or a mouse antibody to STAT-1 (Sc417; Santa Cruz). Bound antibodies were detected by enhanced chemiluminescence (Amersham).
18. See the supplementary material. available on *Science* Online at www.sciencemag.org/cgi/content/full/293/5528/300/DC1.
19. A. Takaoka *et al.*, *Science* **288**, 2357 (2000).
20. EBV-B cells were stimulated with IFN-α or IFN-γ for 2 hours, and total RNA was analyzed by Northern blotting (*4*). The nylon membrane was probed with *P48-*, *MXA-*, or *GDAPH*-specific radiolabeled DNA fragments (available upon request).
21. The *STAT1* cDNA was amplified with sense (5′-TCgACAgTCTTggCACCTAACgTgC-3′) and antisense (5′-TgCTATCAACaggTTgCAgCg-3′) primers. The *STAT1* exon encoding L706 was amplified with sense (5′-TCggTTgATggAAagCgTA-3′) and antisense (5′-CTCTTCTgTgTTCACTTAC-3′) primers. Genomic DNA from various tissues (blood, hair roots, and buccal cells) and cell lines (EBV-B cells and SV40 fibroblasts) was amplified. The products were sequenced as previously described (*10*).
22. The patient was not vaccinated with BCG and had benign illnesses caused by cytomegalovirus and varicella-zoster virus, as attested by serum-specific IgG antibodies.
23. Two days after electroporation with pcDNA3-WT-STAT-1 (provided by M. J. Holtzman), pcDNA3-L706S-STAT-1, or a mock vector, mouse STAT-1–deficient embryonic fibroblasts were stimulated with murine IFN-γ (R&D) or IFN-α (Gibco BRL) for 30 min. Indirect immunofluorescence, with a mouse monoclonal antibody to human STAT-1 (N-Terminus; Transduction Laboratories) or a rabbit antibody specific to STAT-1–phosphotyrosine 701 (9171L; New England Biolabs) was performed as in (*18*). Double immunofluorescence was performed by incubation with a mouse antibody to human STAT-1 (N-Terminus; Transduction Laboratories) and a rabbit antibody to mouse STAT-2 Ab (provided by C. Schindler) for 30 min, followed by a tetramethyl rhodamine isothiocyanate–conjugated mouse antibody (Jackson) and FITC-conjugated rabbit antibody (Jackson) for 30 min as described by C. Park *et al.* [*Nucleic Acids Res.* **27**, 4191 (1999)]. The cells were visualized by confocal microscopy (Zeiss).
24. X. Chen *et al.*, *Cell* **93**, 827 (1998).
25. S. A. Qureshi, S. Leung, I. M. Kerr, G. R. Stark, J. E. Darnell Jr., *Mol. Cell. Biol.* **16**, 288 (1996).
26. R. Kamijo *et al.*, *J. Exp. Med.* **178**, 1435 (1993).
27. U. Muller *et al.*, *Science* **264**, 1918 (1994).
28. M. F. van den Broek, U. Muller, S. Huang, R. M. Zinkernagel, M. Aguet, *Immunol. Rev.* **148**, 5 (1995).
29. J. E. Durbin, R. Hackenmiller, M. C. Simon, D. E. Levy, *Cell* **84**, 443 (1996).
30. M. A. Meraz *et al.*, *Cell* **84**, 431 (1996).
31. M. P. Gil *et al.*, *Proc. Natl. Acad. Sci. U.S.A.*, **98**, 6680 (2001).
32. C. Park, S. Li, E. Cha, C. Schindler, *Immunity* **13**, 795 (2000).
33. We thank L. Abel, S. Pellegrini, J. Puck, and J. C. Weill for helpful discussions and M. J. Holtzman, D. Frank, D. Recan, and C. Schindler for providing cells or reagents. J.-L.C. would like to thank A. Munnich for support and encouragement. This work was supported by grants from Action Incitative Concertée Blanche, Banque Nationale de Paris-Paribas, Fondation pour la Recherche Médicale, Fondation Schlumberger, Legs Poix, Programme National de Recherche Fondamentale en Microbiologie, Maladies Infectieuses et Parasitaires, and Institut Universitaire de France.

29 March 2001; accepted 7 June 2001

Interferon-γ–Mediated Site-Specific Clearance of Alphavirus from CNS Neurons

Gwendolyn K. Binder and Diane E. Griffin*

Recovery from viral encephalomyelitis requires immune-mediated noncytolytic clearance from neurons by mechanisms assumed to be the same for all neurons. In alphavirus encephalomyelitis, antibody clears infectious virus from neurons in all regions of the central nervous system (CNS), but CD8 T cells contribute to elimination of viral RNA. To understand the role of T cells in clearance, we infected antibody knockout mice with Sindbis virus. Virus was cleared from spinal cord and brain stem neurons, but not from cortical neurons, and required both CD4 and CD8 T cells. Infection with cytokine-expressing recombinant viruses suggested that T cells used interferon-γ, but not tumor necrosis factor α, in clearing virus and that populations of neurons differ in responsiveness to this effector pathway.

Viral infections of brain and spinal cord neurons necessitate development of an immune response within the central nervous system (CNS). However, local infiltration of inflammatory cells provides the potential for immune-mediated neurologic damage. Because recovery from viral encephalitis can occur without permanent neurologic damage, noncytolytic mechanisms of clearance must exist. To investigate these mechanisms, we studied a model of murine encephalomyelitis induced by infection with Sindbis virus (SV), a mosquito-borne alphavirus related to western and eastern equine encephalitis viruses. SV infects neurons in both the brain and spinal cord (*1*) and induces a well-characterized immune response in the CNS (*2–4*) that results in clearance of infectious virus within 7 to 8 days without paralysis or death. Thus, SV encephalomyelitis provides an excellent model for identifying the immune mechanisms responsible for effective noncytolytic clearance of virus from the CNS.

Previous studies that used passive transfer of antibody into severe combined immune deficiency (SCID) mice persistently infected with SV showed that antibody is a primary mediator of noncytolytic clearance of infectious virus from neurons in both the brain and spinal cord (*3*). However, antibody-independent cytolytic and noncytolytic T cell–mediated control of virus replication occurs in nonneural tissues (*5–7*). Such mechanisms have been considered irrelevant to virus clearance from neurons, in part because of the restricted expression of major histocompatibility class I and class II antigens by these cells (*8*). Consistent with this view, clearance of infectious SV from neurons is normal in mice deficient in CD8 T cells. However, clearance of viral RNA is slowed in these mice, suggesting an auxiliary role for T cells (*9*).

To investigate whether alternate mechanisms of noncytolytic viral clearance exist, we infected C57BL/6 antibody knockout (μMT) mice (*10*) with the TE strain of SV (*11*) and examined clearance of infectious virus from the brain and spinal cord. As controls, immunocompetent wild-type C57BL/6 and immunodeficient SCID mice (Fig. 1, A and B) were infected with the same SV strain (*12*). Initial levels of virus replication were similar in all mice, and, although wild-type mice cleared infectious virus from the brain and spinal cord between days 6 and 9 after infection, SCID mice established persistent infection in the brain and spinal cord but developed no neurological symptoms. During the first 2 weeks of infection, virus titers in brains of μMT mice were intermediate between those of SCID and wild-type mice, but later, titers were similar to those of SCID mice. In contrast, infectious virus was completely cleared from the spinal cords of μMT mice with a time course that was only slightly slower than that of wild-type mice.

W. Harry Feinstone Department of Molecular Microbiology and Immunology, Johns Hopkins University Bloomberg School of Public Health, Baltimore, MD 21205, USA.

*To whom correspondence should be addressed. E-mail: dgriffin@jhsph.edu

None of the mice showed signs of paralysis, and no loss of motor neurons was observed in μMT animals (Web fig. 1) (*13*) even though they had been infected (Fig. 2E). Therefore, site-specific noncytolytic mechanisms, other than antibody, can clear virus from the CNS.

To determine the role of T cells in virus clearance, we depleted μMT mice of CD4, CD8 (Fig. 1, C and D), or both T cell subsets together (Fig. 1, E and F) (*14*). Depletion of either CD4 or CD8 T cells diminished the reduction of virus levels in the brain and lengthened the time it took to clear infectious virus from the spinal cord. Depletion of CD4 and CD8 T cells together abrogated both initial control of replication in the brain and clearance of virus from the spinal cord. These data indicated that T cells were responsible for clearance of virus in the absence of antibody and that both CD4 and CD8 T cells participated in this process.

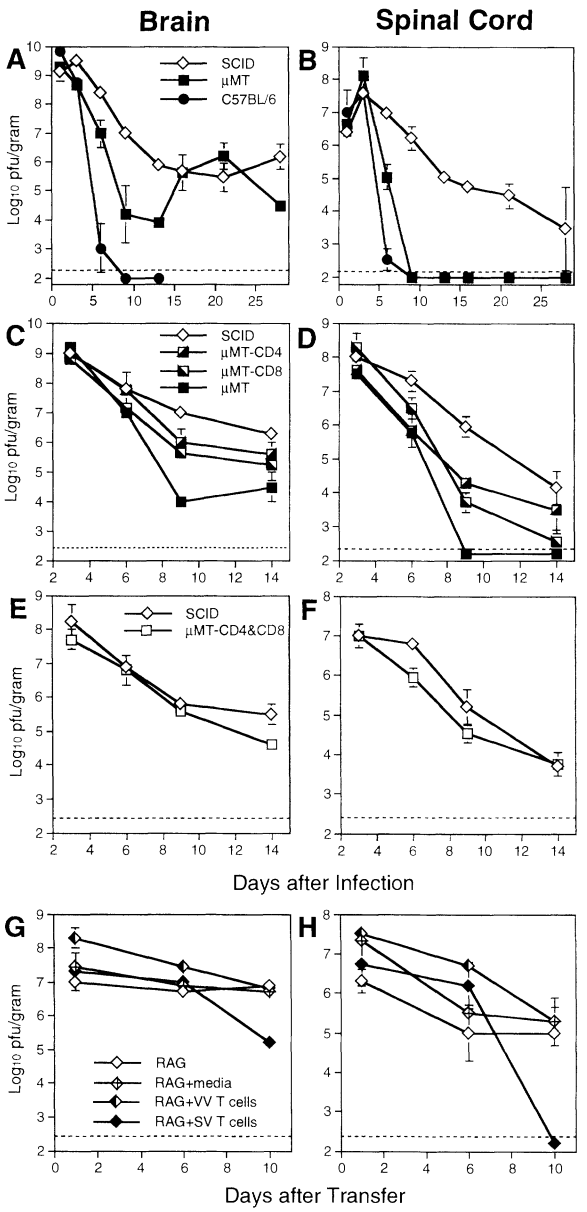

Fig. 1. Clearance of infectious virus in brain and spinal cord. (**A** and **B**) Virus titer in the brain and spinal cord of wild-type, antibody knockout (μMT), and SCID mice is shown and is one of three experiments. (**C** and **D**) Effect of CD4 or CD8 T cell depletion on virus titer in the brain and spinal cord of μMT compared with SCID mice. (**E** and **F**) Effect of CD4 and CD8 T cell depletion together on virus titer in the brain and spinal cord of μMT compared with SCID mice. No data points except day 6 spinal cord (P = 0.024) were significantly different by t test. (**G** and **H**) Ability of VV- or SV-immune T cell transfer, media transfer, or no transfer to reduce virus titer in the brain and spinal cord of RAG knockout mice persistently infected with SV. Infectious virus was quantitated by plaque assay. The dashed line represents the limit of virus detection, and symbols below it indicate no detection. n = 3 at each time point. Error bars represent SEM for (A) to (H).

To establish that T cells are sufficient to clear virus and test whether T cell–mediated clearance is antigen-dependent, we isolated T cells from vaccinia virus– (VV) or SV-immunized μMT mice and transferred them to persistently infected immunodeficient recombination activating gene-1 (RAG) knockout mice (*15*) (Fig. 1, G and H). Transfer of VV-specific lymphocytes or media had no effect on virus, whereas transfer of SV-specific lymphocytes reduced virus in the brain and completely cleared infectious virus from the spinal cord. Previous failed attempts to clear virus from the CNS of SCID mice by passive transfer of T cells may have resulted from transfer of inadequate numbers of activated antiviral T cells (*3*). Thus, although T cells were able to mediate antigen-specific clearance of virus from spinal cord neurons, those of the brain appeared to be relatively resistant to T cell–mediated clearance.

This site-specific difference in viral clearance could be attributable to differences in virus spread, local variation in immune responses, and/or distinct capacities of infected neurons to respond to immune mediators. In situ hybridization for SV RNA revealed widely disseminated infection throughout the brain and spinal cord (Fig. 2, A through F). Immunostaining showed CD4 and CD8 T cell infiltration into the parenchyma of both brain and spinal cord (Fig. 2, G through J). This was reflected by a similar number of T cells per mm^2 in inflammatory foci of the brain and spinal cord (Fig. 2, K and L). T cell activity assessed by ribonuclease (RNase) protection for the cytokines tumor necrosis factor–α (TNF-α), interferon-γ (IFN-γ), interleukin-6 (IL-6), and lymphotoxin-β (LT-β) showed similar expression in brain and spinal cord, suggesting unbiased T cell cytokine production in these regions (Fig. 2, M through P). These data suggested that site-specific clearance reflected variation in the response of different populations of neurons to T cells.

Cells infected in the spinal cord are primarily motor neurons, whereas populations are more diverse in the brain (*16*, *17*). To examine whether control of virus replication differed between brain regions, we infected μMT mice and separately assayed the cortex, cerebellum, brain stem, hippocampus, and spinal cord for clearance of infectious virus (Table 1). Virus levels were below detection in the brain stem and spinal cord, but not in the cortex and hippocampus, indicating that T cell–mediated clearance of virus from the

Table 1. Virus titers in distinct brain regions and spinal cord. μMT mice were infected with SV or SV-CAT. SCID mice were infected with SV-CAT or SV–IFN-γ. Fourteen days later, the cortex, cerebellum, hippocampus, brain stem, and spinal cord were excised and assayed individually for infectious virus, and geometric mean titers ± SEM were calculated (n = 3). The limit of detection was 3.2. ND indicates no detection of infectious virus in any of the mice.

Region	μMT-SV	μMT-SV-CAT	SCID-SV-CAT	SCID-SV–IFN-γ
Cortex	3.8 (±0.29)	3.65	4.44 (±0.31)	4.09 (±0.20)
Hippocampus	4.33 (±0.75)	4.10 (±1.53)	4.79 (±0.41)	4.09 (±0.78)
Cerebellum	ND	ND	ND	ND
Brain stem	ND	ND	3.86 (±0.49)	3.48 (±0.26)
Spinal cord	ND	ND	3.56 (±0.34)	ND

brain was site-dependent. These data complement observations of site-specific immune regulation and sensitivity of the blood brain barrier to cytokines (*18*, *19*) by showing that response of neurons to immune effectors is also site-specific.

The fact that both CD4 and CD8 T cells can mediate clearance of virus (Fig. 1, C through F) suggests either that there are multiple T cell–mediated mechanisms of clearance or that the relevant mechanism is shared by both CD4 and CD8 T cells. Because clearance did not result in neurological damage, we hypothesized that cytokines produced by CD4 or CD8 T cells, rather than a cytotoxic effector response, were most likely to be involved. Two cytokines that have direct antiviral activity (*5*, *7*) and are produced in μMT animals during infection (Fig. 2, K and L) are TNF-α and IFN-γ.

To investigate the antiviral activity of these cytokines in the CNS, we generated recombinant SVs that expressed murine TNF-α (SV–TNF-α), IFN-γ (SV–IFN-γ), or chloramphenicol acetyltransferase (SV-CAT). These genes were inserted into a clone of the TE strain of SV engineered to contain a second subgenomic promoter for foreign protein expression (*20*). The biological activity of the cytokines produced by these viruses was confirmed in an L-929 murine fibroblast cell assay, and replication in cultured cells was equivalent (Web fig. 2) (*13*). Production of cytokine RNA in vivo was confirmed by RNase protection assay. SCID mice were infected with these cytokine-expressing viruses, and levels of virus in brain and spinal cord were compared with those of μMT and SCID mice infected with SV-CAT (Fig. 3). μMT mice cleared virus from the spinal cord and partially controlled replication in the brain, whereas SCID mice infected with SV-CAT became persistently infected, as previously observed with SV (Fig. 1, A and B).

SCID mice infected with SV–TNF-α did not clear virus from the spinal cord, and virus titers were consistently higher than SV-CAT controls in both brain and spinal cord (Fig. 3). Increased virus replication may reflect the ability of TNF-α to break down the blood brain barrier and facilitate virus spread or may suggest a synergistic role for TNF-α in alphavirus replication in the CNS. Although TNF-α exhibits direct antiviral activity in some nonneural tissues (*5*, *7*), it is not sufficient for clearance of virus from neurons infected with mouse hepatitis virus (*21*) or SV.

SCID mice infected with SV–IFN-γ showed reduced amounts of virus in brain and clearance of virus from the spinal cord, paralleling that seen in μMT mice infected with SV-CAT (Fig. 3), and the site dependence of clearance was similar to that observed in μMT mice (Table 1). IFN-γ RNA,

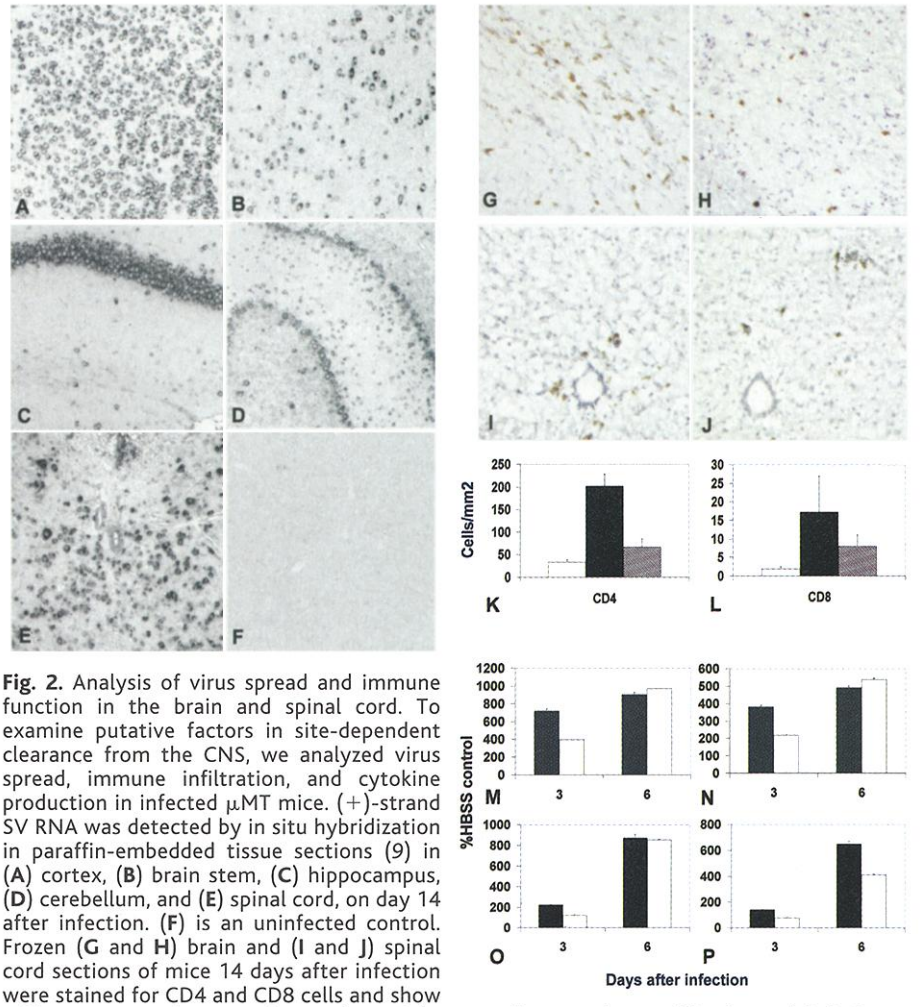

Fig. 2. Analysis of virus spread and immune function in the brain and spinal cord. To examine putative factors in site-dependent clearance from the CNS, we analyzed virus spread, immune infiltration, and cytokine production in infected μMT mice. (+)-strand SV RNA was detected by in situ hybridization in paraffin-embedded tissue sections (*9*) in (**A**) cortex, (**B**) brain stem, (**C**) hippocampus, (**D**) cerebellum, and (**E**) spinal cord, on day 14 after infection. (**F**) is an uninfected control. Frozen (**G** and **H**) brain and (**I** and **J**) spinal cord sections of mice 14 days after infection were stained for CD4 and CD8 cells and show infiltration into the parenchyma. (G and I) CD4 cells were detected by biotin-labeled L3T4 antibody (Pharmingen) and avidin-peroxidase kit (Vector Laboratories). (H and J) CD8 cells were detected by biotin-labeled Ly-2 antibody (Pharmingen) and tyrimide signal amplification (NEN–Life Science Products). Cells were visualized with 3,3′-diaminobenzidine as a chromagen with hematoxylin for counterstain. (A) to (J) are representative of three mice. Quantitation of (**K**) CD4 and (**L**) CD8 T cells per mm^2 tissue was performed to show relative levels of infiltration. Open bars represent T cell counts over the whole brain area, closed bars represent averaged T cell counts in inflammatory foci from cortex and hippocampus, and hatched bars represent T cell counts in spinal cord. Open and closed bars on day 3 were significantly different ($P = 0.03$) by t test, but no other significant differences were observed. Production of (**M**) TNF-α, (**N**) IFN-γ, (**O**) IL-6, and (**P**) LT-β in brain (closed bars) and spinal cord (open bars) was detected by RNase protection analysis with the Mck-3B template set, kit, and protocol (Pharmingen). Results are presented as percentage of buffer-infected control. Differences were not significant by t test. $n = 3$ and error bars represent SEM for (K) to (P).

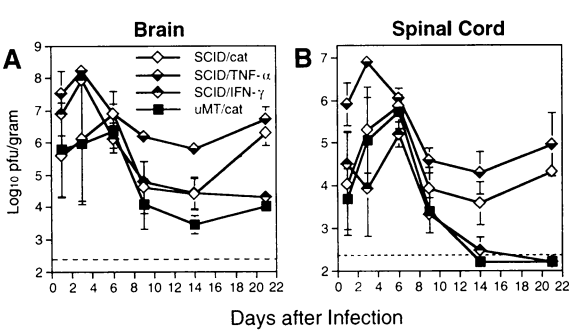

Fig. 3. IFN-γ, but not TNF-α, mediates site-specific virus clearance. SCID mice were infected with SV-CAT, SV–TNF-α, and SV–IFN-γ. μMT mice were infected with SV–IFN-γ, SV–TNF-α, and SV-CAT. Virus was quantitated in (**A**) brain and (**B**) spinal cord. Symbols falling below the limit of detection (dashed line) indicate no detection of infectious virus. $n = 5$ for days 1 to 6, $n = 6$ for days 9 and 14, and $n = 3$ for day 21 after infection. Error bars represent SEM. Data from days 1 to 3 of both brain and spinal cord were not significantly different except for SV–TNF-α and SV–IFN-γ on day 3 in spinal cord ($P = 0.03$ by t test).

analyzed by RNase protection assay, was present in all brain compartments examined (*22*). Approximate extracellular IFN-γ production by recombinant virus is 1.5×10^6 plaque-forming units (pfu) per unit of IFN-γ, as determined by L-929 bioactivity assay. The relative roles of secreted and intracellular IFN-γ in SV clearance are unclear, but previous studies have shown that intracellular IFN-γ can mediate virus protection in an IFN-γ receptor–dependent fashion similar to that of exogenous IFN-γ (*23*). Therefore, local production of IFN-γ alone is sufficient to effect T cell–mediated clearance of virus from some, but not all regions of the CNS. IFN-γ has direct antiviral activity in peripheral tissues and is important for clearance of mouse hepatitis virus from neurons and of VV from choriodal and meningeal cells in vivo (*21*, *24*, *25*). Our data provide further evidence for the specific role of IFN-γ in noncytolytic clearance of virus from some, but not all, types of neurons.

CD8 T cells function through cytokine production and/or the cytotoxic response. It is widely accepted that cytotoxic T lymphocytes (CTL) provide antiviral protection through lysis of infected cells (*26*). However, in situations where the cells are nonrenewable or where large numbers of cells are infected, lysis is counterproductive or not effective. Early studies of persistent lymphocytic choriomeningitis virus infection of the CNS suggested that CD8 T cells could resolve infection without necrosis (*27*), and evidence has accumulated for alternate noncytolytic, cytokine-mediated T cell mechanisms of virus clearance (*6*, *28*, *29*). Our study demonstrates IFN-γ–mediated noncytolytic clearance of virus from neurons in vivo, providing evidence for the role of T cell cytokine production in the resolution of virus infection as an alternative to CTL-mediated killing of virus-infected cells. However, neurons are heterogeneous in their responses to IFN-γ, resulting in a failure to contain virus replication in localized regions of the CNS. These results define some of the important immune components for recovery from viral encephalomyelitis, which could be useful in developing therapies targeted for specific regions of the CNS.

References and Notes

1. A. C. Jackson, T. R. Moench, B. D. Trapp, D. E. Griffin, *Lab. Invest.* **58**, 503 (1988).
2. D. E. Griffin, R. T. Johnson, *J. Immunol.* **118**, 1070 (1977).
3. B. Levine *et al.*, *Science* **254**, 856 (1991).
4. S. L. Wesselingh, D. E. Griffin, *J. Immunol.* **152**, 1289 (1994).
5. L. G. Guidotti, F. V. Chisari, *Virology* **273**, 221 (2000).
6. L. G. Guidotti *et al.*, *Science* **284**, 825 (1999).
7. A. J. Ramsay, J. Ruby, I. A. Ramshaw, *Immunol. Today* **14**, 155 (1993).
8. E. Joly, L. Mucke, M. B. A. Oldstone, *Science* **253**, 1283 (1991).
9. T. Kimura, D. E. Griffin, *J. Virol.* **13**, 6117 (2000).
10. D. Kitamura, J. Roes, R. Kuhn, K. Rajewsky, *Nature* **350**, 423 (1991).
11. P. C. Tucker, D. E. Griffin, *J. Virol.* **65**, 1551 (1991).
12. Wild-type C57BL/6J, antibody knockout C57BL/6-*Igh-6*^{tm1Cgn}, SCID C57BL/6J-*Prkdc*^{scid}/*SzJ*, and recombination activating gene-1 knockout C57BL/6J-*Rag1*^{tm1Mom} were purchased from the Jackson Laboratory at 4 to 6 weeks of age. For infection, 1000 pfu of SV in 30 μl of Hanks' balanced salt solution was injected intracerebrally with a tuberculin syringe.
13. The Web figures are available on *Science* Online at www.sciencemag.org/cgi/content/full/293/5528/303/DC1.
14. The GK1.5 (α-CD4)- and 2.43 (α-CD8)-producing hybridomas (American Type Culture Collection, Manassas, VA) were injected into SCID mice for ascites production, and antibody was quantitated by enzyme-linked immunosorbent assay (Bethyl Laboratories). Mice were given 0.25 mg of antibody in a total of 0.5 ml of phosphate-buffered saline intraperitoneally every day for 3 days. Three days later, depletion was complete (>98%) and mice were infected with SV. Depletion was confirmed for each mouse by flow cytometric analysis of spleen cells.
15. μMT mice were vaccinated in each footpad with either 330 pfu of SV or 2.5×10^4 pfu of VV. Six days later, lymphocytes from draining lymph nodes were removed and suspended in Dulbecco's modified essential medium containing 10% fetal bovine serum and penicillin or streptomycin. SCID mice were infected with SV 3 days before intraperitoneal transfer of 6×10^6 cells.
16. J. P. Kelly, in *Principles of Neural Science*, E. R. Kandel, J. H. Schwartz, T. M. Jessell, Eds. (Elsevier Science, New York, 1991), pp. 283–295.
17. ———, J. Dodd, in *Principles in Neural Science*, E. R. Kandel, J. H. Schwartz, T. M. Jessell, Eds. (Elsevier Science, New York, 1991), pp. 273–282.
18. L. Schnell, S. Fearn, H. Klassen, M. E. Schwab, V. H. Perry, *Eur. J. Neurosci.* **11**, 3648 (1999).
19. L. P. McCluskey, L. Lampson, *J. Neuropathol. Exp. Neurol.* **59**, 177 (2000).
20. E. H. Cheng, B. Levine, L. H. Boise, C. B. Thompson, J. M. Hardwick, *Nature* **379**, 554 (1996).
21. B. D. Pearce, M. V. Hobbs, T. S. McGraw, M. J. Buchmeier, *J. Virol.* **68**, 5483 (1994).
22. G. K. Binder, D. E. Griffin, unpublished data.
23. A. Will, U. Hemmann, F. Horn, M. Rollinghoff, A. Gessner, *J. Immunol.* **157**, 4576 (1996).
24. M. Lin, D. Hinton, S. Stohlman, *Adv. Exp. Med. Biol.* **440**, 431 (1998).
25. T. M. Kundig, H. Hengartner, R. M. Zinkernagel, *J. Immunol.* **150**, 2316 (1993).
26. R. M. Zinkernagel, P. C. Doherty, *Nature* **248**, 701 (1974).
27. M. B. A. Oldstone, P. Blount, P. J. Southern, *Nature* **321**, 239 (1986).
28. I. A. Ramshaw *et al.*, *Immunol. Rev.* **159**, 119 (1997).
29. L. G. Guidotti *et al.*, *Immunity* **4**, 25 (1996).

30. We thank B. Schofield for assistance in imaging and photography. Supported by grants from the Markey Foundation (G.K.B.) and from the National Institute of Neurological Diseases and Stroke (D.E.G.).

9 February 2001; accepted 30 May 2001

Homeostatic Regulation of the Immune System by Receptor Tyrosine Kinases of the Tyro 3 Family

Qingxian Lu and Greg Lemke*

Receptor tyrosine kinases and their ligands mediate cell-cell communication and interaction in many organ systems, but have not been known to act in this capacity in the mature immune system. We now provide genetic evidence that three closely related receptor tyrosine kinases, Tyro 3, Axl, and Mer, play an essential immunoregulatory role. Mutant mice that lack these receptors develop a severe lymphoproliferative disorder accompanied by broad-spectrum autoimmunity. These phenotypes are cell nonautonomous with respect to lymphocytes and result from the hyperactivation of antigen-presenting cells in which the three receptors are normally expressed.

The elimination of reactive lymphocytes is a central feature of homeostatic regulation in the immune system. Although clonal expansion of lymphocytes is essential for immune responses, activated T and B cells must be deleted once the antigens that triggered their expansion have been eradicated. Similarly, autoreactive T cell clonotypes pose a severe threat to tissue and organ integrity, and must also be deleted. Deficiencies in the homeostatic regulation of expanded or autoreactive lymphocytes lead to lymphoproliferative disorders, impaired immune function, autoimmunity, and death (*1*).

In the mature immune system, lymphocyte numbers are under the control of a wide variety of soluble cytokines, as well as cell surface inhibitory and costimulatory molecules. Although many of these regulators bind to receptors that are coupled to cytoplasmic protein-tyrosine kinases (PTKs), none of them is known to signal through the more direct mechanism of binding and activating a receptor with intrinsic PTK activity (*2*). This notwithstanding, we have found that three structurally related receptor PTKs—Tyro 3 (*3*, *4*), Axl (*3*, *5*), and Mer (*3*, *6*)—play an essential immunoregulatory role. These receptors are, together with their ligands Gas6

Molecular Neurobiology Laboratory, The Salk Institute, La Jolla, CA 92037, USA.

*To whom correspondence should be addressed. E-mail: lemke@salk.edu